Environmental Science and Pollution Research (2019) 26:20581–20594
https://doi.org/10.1007/s11356-019-05383-9

RESEARCH ARTICLE

Ovariectomy predisposes female rats to fine particulate matter exposure's effects by altering metabolic, oxidative, pro-inflammatory, and heat-shock protein levels

Pauline Brendler Goettems-Fiorin[1,2] · Lilian Corrêa Costa-Beber[1,3] · Jaíne Borges dos Santos[1] · Paula Taís Friske[1] · Lucas Machado Sulzbacher[1] · Matias Nunes Frizzo[1,3] · Mirna Stela Ludwig[1,3] · Cláudia Ramos Rhoden[2] · Thiago Gomes Heck[1,3]

Received: 26 December 2018 / Accepted: 3 May 2019 / Published online: 18 May 2019

Abstract

The reduction of estrogen levels, as a result of menopause, is associated with the development of metabolic diseases caused by alterations in oxidative stress (OS), inflammatory biomarkers, and 70-kDa heat-shock protein (HSP70) expression. Additionally, exposure to fine particulate matter air pollution modifies liver OS levels and predisposes organisms to metabolic diseases, such as type 2 diabetes (T2DM). We investigated whether ovariectomy affects hepatic tissue and alters glucose metabolism in female rats exposed to particulate air pollution. First, 24 female Wistar rats received an intranasal instillation of saline or particles suspended in saline 5 times per week for 12 weeks. The animals then received either bilateral ovariectomy (OVX) or false surgery (sham) and continued to receive saline or particles for 12 additional weeks, comprising four groups: CTRL, Polluted, OVX, and Polluted+OVX. Ovariectomy increased body weight and adiposity and promoted edema in hepatic tissue, hypercholesterolemia, glucose intolerance, and a pro-inflammatory profile (reduced IL-10 levels and increased IL-6/IL-10 ratio levels), independent of particle exposure. The Polluted+OVX group showed an increase in neutrophils and neutrophil/lymphocyte ratios, decreased antioxidant defense (SOD activity), and increased liver iHSP70 levels. In conclusion, alterations in the reproductive system predispose female organisms to particulate matter air pollution effects by affecting metabolic, oxidative, pro-inflammatory, and heat-shock protein expression.

Keywords Air pollution · Menopause · Estrogen · Metabolic diseases · Heat shock proteins · Oxidative stress · Inflammation

Introduction

Women have an estimated life expectancy of 72–82 years, and there were at least 1.1 billion postmenopausal women globally as recently as 2011 (North American Menopause Society 2010). Since most postmenopausal women live in the cities of developing countries with higher levels of air pollution emission (Yu et al. 2018), many postmenopausal women experience chronic air pollution exposure. The loss of ovarian function and, subsequently, low estrogen levels in menopause is associated with the development of cardiovascular and metabolic diseases, such as type 2 diabetes mellitus (T2DM), and may aggravate the senescence process via an increase in generalized inflammation (Benedusi et al. 2014). Since estrogen regulates multiple functions in various organs, cells, and genes (Rettberg

Responsible editor: Philippe Garrigues

✉ Pauline Brendler Goettems-Fiorin
pauline.goettems@unijui.edu.br

✉ Thiago Gomes Heck
thiago.heck@unijui.edu.br

[1] Research Group in Physiology, Department of Life Sciences, Regional University of Northwestern Rio Grande do Sul State (UNIJUÍ), Rua do Comércio, 3000 – Bairro Universitário, Ijuí, RS 98700-000, Brazil

[2] Atmospheric Pollution Laboratory, Postgraduate Program in Health Sciences, Federal University of Health Sciences of Porto Alegre (UFCSPA), Rua Sarmento Leite, 245, Porto Alegre, RS, Brazil

[3] Postgraduate Program in Integral Attention to Health (PPGAIS-UNIJUÍ/UNICRUZ), Ijuí, RS, Brazil

et al. 2014), a decline in circulating estrogen levels may increase cardiovascular risk by effects related to increased adiposity and impaired lipid metabolism (Schneider et al. 2006). Hence, almost two-thirds of menopausal women are overweight or obese and have vasomotor problems, with a high prevalence of hypertension and T2DM (Santos et al. 2012). Experimental (Goettems-Fiorin et al. 2016; Liu et al. 2014; Xu et al. 2010) and epidemiological evidence (Pearson et al. 2010) has also shown that environmental air pollution is associated with the development of metabolic diseases and is related to worsening metabolic dysfunction, suggesting that pathophysiological effects caused by air pollution exposure may be more severe in individuals who are already compromised.

Air pollution is considered a cause of many diseases attributed to environmental factors, causing an estimated 3.1 million pollution-related deaths per year (Miller et al. 2012). Of the pollutants found in urban areas, fine particulate matter ($PM_{2.5}$), a complex mixture of organic and inorganic substances (Who 2003) with an aerodynamic size of less than 2.5 μm, has the greatest health impact. The main sources of $PM_{2.5}$ are combustive emissions from industry and particles formed in vehicle emissions. Residual oil fly ash (ROFA), a metal-rich environmental $PM_{2.5}$, from engines has been used in animal or in vitro studies to evaluate the mechanisms involved in the development of many diseases related to $PM_{2.5}$ exposure (Sacks et al. 2011).

The elderly, infants, and persons with chronic cardiopulmonary diseases are considered to be most susceptible to the mortality and morbidity effects of air pollution exposure (Pope 2000). Thus, people with T2DM exposed to $PM_{2.5}$ present a higher risk of metabolic impairment, as well as the oxidative effects of $PM_{2.5}$ (Goettems-Fiorin et al. 2016; Pearson et al. 2010; Sun et al. 2009). In human and animal studies, inflammation, oxidative stress, and 70 kDa heat-shock protein (HSP70) imbalance are described as mechanisms of impaired glucose homeostasis, mainly due to liver injury and dysfunction (Cangeri Di Naso et al. 2015). Similarly, cumulative evidence has shown that estrogen loss in menopause is associated with the development of metabolic diseases (Lizcano and Guzmán 2014) by mechanisms related to increased oxidative stress (Oliveira et al. 2018), inflammation, and impaired HSP70 balance (Crist et al. 2009; Heck et al. 2017). Furthermore, high plasma HSP70 levels represent a warning signal and oxidative biomarker under environmental challenges that can be used as a subclinical biomarker of the effects of environmental pollutant exposure (Baldissera et al. 2018). In this study, we investigated whether low estrogen levels affect hepatic tissue and alter glucose metabolism in female rats exposed to particulate air pollution.

Materials and methods

Animals

Female 8-week-old Wistar rats ($n = 24$) from the Regional University of the Northwestern Rio Grande do Sul State (UNIJUÍ) animal facility were kept under controlled temperature (24 ± 2 °C) and light-dark cycle (light from 7:00 a.m. to 7:00 p.m.) conditions. The animals received water and food ad libitum. This protocol was approved by the Animal Ethics Committee of UNIJUÍ (CEUA 076/15).

Experimental design

The rats ($n = 24$) were randomly assigned to two groups that received either an intranasal instillation of 50 μL of saline daily for 12 weeks (representing a clean environment) or particles suspended in saline (250 μg, representing a polluted environment) (Fig. 1, white background). Next, the animals received either ovariectomy (OVX) or false surgery (Sham) and continued to receive saline or particles for 12 additional weeks, comprising four groups: animals that received saline and received sham surgery (CTRL, $n = 6$) or ovariectomy (OVX, $n = 6$) and animals that received particles and were submitted to sham surgery (Polluted, $n = 6$) or ovariectomy (Polluted+OVX, $n = 6$) (Fig. 1, gray background). Throughout the study, biometric and consumption profiles, as well as glycemia and glucose tolerance tests, were performed every 4 weeks. After 24 weeks, the animals were euthanized, and blood and tissue were collected for biochemical and molecular analysis.

Particulate matter—particle characterization

Residual oil fly ash (ROFA) particles were collected from an electrostatic precipitator installed in the chimney of a large steel factory located in São Paulo (SP, Brazil). Animals in the polluted group received a daily intranasal dose (between 4:00 and 5:00 p.m.) of 50 μL of the ROFA suspension at the concentration of 5 μg/μL 5 days per week over a 24-week period, for a total daily dose of 250 μg. Since chronic exposure can be defined as repeated exposure via the inhalation route for more than 90 days is typical in laboratory studies using animal species (EPA 2010), we consider our chronic particle exposure regimen to be adequate. Control groups received 50 μL of a saline solution. The intranasal administration process was performed using an automatic pipette to deliver 50 μL of the solution into the animal's nostril; this procedure triggers the apnea reflex, which promotes the inhalation of the pollutant (Medeiros et al. 2004). The particles used in this study consist of Pb (3.1 ± 0.09), Al (789 ± 23), Zn (20.3 ± 0.04), Cd (0.04 ± 0.002), Ba (30.2 ± 0.31), Cu (9.7 ± 0.1), Ni (287 ± 10.8), As (4.1 ± 0.05), Se (7.5 ± 0.20), Mn

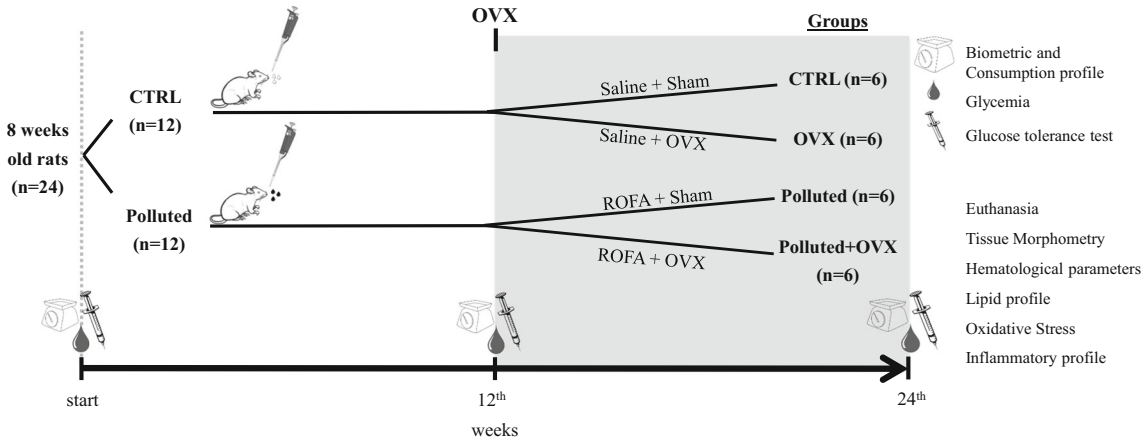

Fig. 1 Female Wistar rats were randomly assigned to receive either an intranasal dose of saline (representing a clean environment; CTRL) or ROFA particles suspended in saline (250 μg, representing a polluted environment, Polluted) daily for 12 weeks (white box). The animals then received either ovariectomy or sham surgery and continued to receive saline or ROFA for an additional 12 weeks (gray box), comprising four groups: animals that received saline and received either sham surgery (CTRL) or ovariectomy (OVX) and animals that received ROFA and received either sham surgery (Polluted) or ovariectomy (Polluted+OVX). Throughout the study, biometric and consumption profiles were collected, and glycemia and glucose tolerance tests were performed every 4 weeks. After 24 weeks, the animals were euthanized, and blood and tissue were collected for biochemical and molecular analysis

(48.3 ± 0.98), Sr (8.4 ± 0.16), Sb (2.3 ± 0.57), Fe (20,397.2 ± 283.3), Mg (372.5 ± 1.93), P (388.5 ± 255.8), and Cr (7.6 ± 0.23) (mean ± SD, expressed by ng per m^3 of air). The particles have an average aerodynamic diameter of 1.2 ± 2.2 μm.

Ovariectomy

The animals were submitted to a surgical protocol. First, a preanesthetic medication, consisting of 5 mg/kg morphine intraperitoneal (i.p.), was administered. Next, 4% isofluorane (BioChimico®) was administered to induce anesthesia, followed by 2% isofluorane (BioChimico®) to maintain anesthesia. OVX corresponds to the bilateral removal of the ovaries and is achieved by a longitudinal incision in the lateral region of the abdomen, close to the hind limbs. The non-ovariectomized animals were submitted to false operation (Sham) where their ovaries were identified and surgically exposed and then repositioned for posterior suturing of the musculature and skin. After the surgical procedure, all animals (Sham and OVX) received appropriate postoperative treatment, which included body temperature and pain signal monitoring, in addition to pharmacological treatment: meloxicam (Ouro Fino®) 0.2% (2 mg/kg, subcutaneously) after 24 h (single dose).

Food and water consumption

The animals' water and food consumption, as determined by the volume of water offered minus the remaining volume in the bottle (mL) and the amount of food provided minus the remaining food in the box (g), was monitored 3 times per week during the 24-week study.

Biometric profiles and tissue morphometry

Each animal's biometric profile was monitored once every 4 weeks during the 24-week study. Body weight (g) and length (cm) measurements were taken and used to calculate a Lee index value (Lee 1929). The rats' body weight was checked with a semi-analytical scale, and their length was verified by naso-anal distance. The Lee index consists of dividing the cube root of the animal's body weight (g) by naso-anal distance (cm) (Lee 1929). At the end of the study, we also evaluated adiposity (i.e., % of visceral white adipose tissue [WAT]/body weight) and percent of the liver, pancreas, gastrocnemius, and soleus muscle weight in relation to body weight. Visceral white adipose tissue was collected from the perigonadal region surrounding the uterus and ovaries for analysis. Pulmonary and hepatic edema was evaluated using the wet/dry weight ratio.

Glycemia and the glucose tolerance test

Blood glucose levels were monitored before the start of the interventions, before the surgical procedure (12ª week), and at the end of the study (24ª week). Blood glucose was measured by Glucometer Optium Xceed (Abbott®) (5 μL of tail blood) after 12 h of fasting. A glucose tolerance test was performed before the start of the interventions and at the 12th and 24th weeks of intervention in all animals. Food was withdrawn 12 h before the GTT. Glycemia was measured as described above immediately before and at 15, 30, and 120 min after glucose (1 g/kg in saline solution, *i.p.*) administration. The glycemic response during glycemia and the glucose tolerance

test (GTT) was evaluated via the area under the curve (AUC) method (Who 1998).

Blood collection and tissue preparation

At the end of the 24-week intervention, the animals were euthanized, and whole blood was immediately collected and stored in a vial containing 2 mg/mL of ethylenediaminetetraacetic acid (EDTA) anticoagulant for aliquots of total blood (blood count) and plasma (evaluation of IL-6, IL-10, and eHSP70). Blood was collected without EDTA to obtain serum used to obtain a lipid profile and determine the 17β-estradiol concentration. Each blood sample was centrifuged at 3000 rpm for 15 min, and plasma was frozen with PMSF (Phenyl Methyl Sulfonyl Fluoride, Sigma® P7626, FW = 174.19 g/mol; 1.74 mg/mL = 100 mM) for the subsequent measurement of IL-6, IL-10, and eHSP70. The remainder was used for the aforementioned hematological analyses.

Metabolic-related tissues (MRT; i.e., WAT, liver, pancreas, gastrocnemius, and soleus muscle) were dissected and weighed. The liver was freeze-clamped in liquid nitrogen and stored for further homogenization. For the analysis of oxidative stress (i.e., thiobarbituric acid reactive substances (TBARS), antioxidant activity enzymes, superoxide dismutase (SOD), and catalase (CAT)), a portion of the liver was homogenized in a potassium phosphate buffer (KPi) pH 7.4. Another portion of the tissue was homogenized in a 0.1% (*w*/*v*) sodium dodecyl sulfate (SDS) buffer to determine iHSP70 expression by Western blotting.

The liver was homogenized (still frozen) in respective buffers, containing a protease inhibitor (PMSF—phenylmethyl-sulfonyl fluoride, 100 μM). Afterward, the homogenates were centrifuged for 10 min at room temperature, and the supernatant fractions were used for Bradford protein determination (Bradford 1976) using bovine serum albumin, as standard.

The measurement of 17β-estradiol (E2)

To determine17β-estradiol (E2) levels, a serum sample was used, and a quantitative dosage was made through the automated system ADVIA Centaur XP® (Siemens Healthcare Diagnosis) by chemiluminescence methodology with sensitivity and in vitro test limits between 20 and 3000 pg/mL.

Hematological parameters

The blood was conditioned in an anticoagulant tube (EDTA) to determine hematological parameters (5 μL of EDTA for each 500 μL of blood) as previously described. For automatic determination, the hematology analyzer Micros 60® (Horiba) was used. Using this equipment, the following parameters can be obtained: the total red blood cell count, hematocrit, hemoglobin, hematimetric indexes (VCM, HCM, and CHCM), erythrocyte distribution range—RDW; total counts of leukocytes, relative and absolute counts of leukocytes (neutrophils, eosinophils, basophils, lymphocytes, and monocytes), and platelet counts (Horiba-User Manual).

Samples were diluted 1:2 with 0.9% saline and analyzed in triplicate. Next, blood smear were performed on a blade, stained with panoptic staining (Newprov®), and analyzed by a professional, who counted 100 cells per sample.

To obtain the neutrophil-to-lymphocyte ratio (NLR), the number of neutrophils was divided by the number of lymphocytes, and to obtain platelet/lymphocyte ratio (PLR), the number of platelets was divided by the number of lymphocytes.

Lipid profiles

Triglycerides, total cholesterol, and lipoproteins (HDL-C) were performed by colorimetric methods with direct dosages. To obtain values related to the variables of the lipid profile, 100 μL of serum per animal and 250 μL of reagent were used for each analysis. Bioclin-Quibasa kits were used to perform these analyses using BS200 - Mindray® automation. The LDL-C dosage was estimated by the Friedewald formula (LDL-C = CT-HDL-C-TG / 5), where TG/5 represents the cholesterol bound to VLDL-C (Sposito et al. 2001).

Liver triglyceride content

Lipids from liver samples (50 mg) were extracted in 1 mL isopropanol. After centrifugation, to perform an enzymatic colorimetric determination of the triglyceride concentration, 10 μL of the supernatant aliquots was added to 500 μL of a reagent (Labtest®) (Oakes et al. 2001). The results were expressed in gram of lipids/100 g of liver tissue.

Oxidative stress, inflammatory profiles, and HSP70 content

Lipid peroxidation

Liver lipid peroxidation concentrations were analyzed using the thiobarbituric acid reactive substances method (TBARS; Buege and Aust 1978). Homogenates were precipitated with 10% trichloroacetic acid, centrifuged, and incubated with thiobarbituric acid for 15 min at 100 °C. Then, the absorbance was measured at 535 nm. The MDA standard was prepared from 1.1.3.3-Tetramethoxypropane (concentrations between 0.0005 and 0.016 mg/mL). The results were expressed in mmol MDA/mg of protein.

SOD and CAT activity

Liver SOD activity was analyzed by inhibiting the auto-oxidation of pyrogallol procedure (Marklund and Marklund 1974). Briefly, in a cuvette, 954 μL of 50 mM Tris/1 mM EDTA buffer (pH 8.2), 4 μL of catalase (CAT; 30 μM), 10 μL of homogenate, and 32 μL pyrogallol (24 mM in HCl 10 mM) were added and mixed. SOD activity was determined at 36 °C in a spectrophotometer (420 nm) every 20 s for 120 s. Results were expressed in units of SOD/mg of protein.

Liver CAT activity was analyzed by the decomposition of hydrogen peroxide procedure (Aebi 1984). In a quartz cuvette, 955 μL of phosphate buffer (50 mM, pH 7.4) and 35 μL of hydrogen peroxide (0.01 M) were mixed. Then, 10 μL of homogenate was added and mixed. CAT activity was determined at 36 °C in a spectrophotometer (240 nm) every 15 s for 120 s. The results were expressed in units of CAT/mg of protein.

Cytokines (IL-10 and IL-6) levels

Plasma and liver levels of IL-6 and IL-10 were measured using an ELISA kit (RayBio® Rat IL-6 and IL-10, Raybiotech, Inc., USA). The colorimetric optical density was detected at a wavelength of 450 nm. The cytokine levels were calculated based on a standard curve constructed for each assay, and each assay was performed in duplicate. All cytokines were reported as picogram per milliliter.

HSP70 tissue expression (iHSP70)

iHSP70 expression was evaluated in the liver by immunoblot analyses (Kolberg et al. 2006). Equivalent amounts of protein from each sample (~40 μg) were mixed with Laemmli's gel loading buffer (50 mM Tris, 10% [*w*/*v*] SDS, 10% [*v*/*v*] glycerol, 10% [*v*/*v*] 2-mercaptoethanol, and 2 mg/mL bromphenol blue) in a ratio of 1:1, boiled for 5 min, and electrophoresed in a 10% polyacrylamide gel (5 h in 15 mA/gel). The proteins were then transferred onto a nitrocellulose membrane (GE Healthcare) by electrotransfer (1 h in 100 V), and subsequently, transferred bands were visualized with 3% (*w*/*v*) Red Ponceau S (Sigma-Aldrich).

The procedures were performed with a vacuum pump for rapid immunoblot. Membranes were washed with TEN-Tween 20 solution (0.1% *w*/*v*; TEN is 50 mM Tris, 5 mM EDTA, 150 mM NaCl, pH 7.4) and then blocked in 0.5% (*w*/*v*) nonfat dry milk in a washing buffer (TEN-Tween 20 solution). Membranes were incubated for 12 h with the monoclonal anti-HSP70 antibody (Sigma-Aldrich H5147, 1:1000). After three consecutive washings with the washing buffer, peroxidase-labeled rabbit anti-mouse IgG (Sigma-Aldrich A9044) was utilized as a secondary antibody at 1:15000 dilution. As a gel loading control, Coomassie Blue (0.1% Coomassie blue, 40% methanol, 10% acetic acid) detection of 43 kDa β-actin region was used. Blot visualization was performed using ECL-Prime Western Blotting Reagent (GE Healthcare®). Quantification of bands was performed using Image J® software. The data were presented in arbitrary units of iHSP70.

Plasma HSP72 (eHSP72) levels

A highly sensitive EIA method (EKS-715 Stressgen, Victoria, BC, Canada) was used to determine the amount of eHSP72 protein in plasma as previously described (Hou et al. 2010). Absorbance was measured at 450 nm, and a standard curve constructed from known dilutions of HSP72 recombinant protein was used to allow a quantitative assessment of eHSP72 plasma concentrations. Quantification was made using a microplate reader (Mindray MR-96A®). The intra-assay coefficient of variation was identified as being less than 2%.

[eHSP72]/[iHSP70] ratio

After performing eHSP72 (plasma) and iHSP70 (liver) measurements, an extracellular to intracellular HSP70 ratio index (H-index) was established. This index reveals the rats' immunoinflammatory status (Heck et al. 2017). The rationale is that with higher eHSP70 amounts, there are more inflammatory signals because eHSP70 is pro-inflammatory in nature. However, for each particular "j" situation, the more the cells are able to respond to stressful stimuli by enhancing iHSP70 and the more such cells are facing a state of anti-inflammation.

Therefore, if one takes Rc = (eHSP70)c/(iHSP70)c as the HSP70 ratio in a control situation, regardless of the techniques used to assess each eHSP70 and iHSP70, the H-index can be calculated as the quotient of any Rj = (eHSP70)j/(iHSP70)j by Rc, which will, therefore, be considered the unity (CTRL = 1), normalizing all the remaining results in situation "j." Hence, H-index = Rj/Rc may allow for comparisons between any stressful situation "j" and the assumed control condition. The H-index can be applied to estimate an animal's immuno-inflammatory status in many different situations as responses to dietary and environmental challenges are present in each tissue.

Statistical analysis

The statistical analysis included a *t* test, as well as a one- and two-way analysis of variance (ANOVA). Post hoc multiple comparisons among groups were performed with the Tukey's test. All statistical analyses were performed using GraphPad for Windows, version 5.0. The level of significance was set at $P < 0.05$. Results were expressed as mean ± standard error or standard deviation.

Results

The effects of reduced estrogen levels on the weight gain of rats exposed to PM

We evaluated the effects of PM exposure and reduced estrogen levels on the biometric profile of female rats. First, we observed no significant weight gain or loss during the 12-week particle exposure period (left side of Fig. 2a and b, respectively). Second, we observed that ovariectomized rats, which had lower estrogen levels (17β-estradiol levels, CTRL = 34.6 ± 7.4; Polluted = 33.6 ± 11.5; OVX = 23.1 ± 4.1* and Polluted+OVX = 28.6 ± 5.6*, pg/mL; * OVX and Polluted+OVX vs CTRL and Polluted; $P = 0.019$), experienced weight gains during the following 12 weeks (right side of Fig. 2a) when compared with the non-ovariectomized rats. The reduced estrogen levels seem to have induced weight gain in rats previously exposed to particulate matter (PM) (Fig. 2c). No alterations were observed in the rats' body length ($P = 0.685$) or body mass index (Lee index, $P = 0.312$).

To ensure that the amount of food consumed did not influence the weight gain result, we analyzed the rats' food intake behavior and observed that there was no difference between the groups in food consumption (food intake, g/week/animal, CTRL = 43.1 ± 6.5; Polluted = 44.8 ± 6.1; OVX = 43.7 ± 6.4, and Polluted+OVX = 44.9 ± 6.5. $P = 0.947$, $F_{3,20} = 0.119$).

The effects of reduced estrogen levels on the glycemic, lipidemic, and hepatic lipid profile of rats exposed to PM

The rats' glucose tolerance was evaluated prior to any intervention (Fig. 3a, b), after 12 weeks of pollution exposure (before ovariectomy; Fig. 3c, d), and at the end of the study (Fig. 3e, f). All animals presented a similar standard GTT response before the interventions (Fig. 4a, b), but 12 weeks of pollution exposure induced a glucose intolerance profile characterized by higher peak glucose levels in the GTT results (Fig. 3c) and by the area under the GTT curve (Fig. 3d). At the 24th week, the reduced estrogen levels induced glucose intolerance in the rats' GTT response, observed by increased glycemia levels 15 min after glucose administration in the OVX group (Fig. 3e) without alterations in AUC (Fig. 3f).

Reduced estrogen levels promoted an increase in total cholesterol levels (Table 1). No alterations in fasting glycemia, triacylglycerol, HDL-cholesterol, or LDL-cholesterol were observed (Table 1). The interventions also did not promote alterations in hepatic triglyceride content (Table 1).

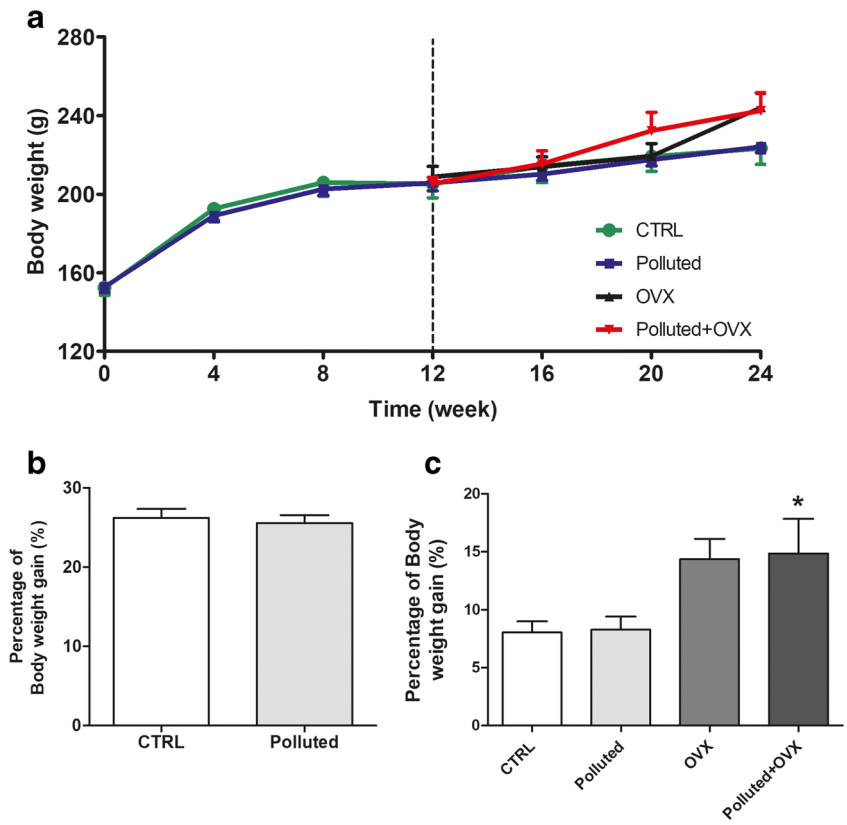

Fig. 2 The effect of reduced estrogen levels on body weight in animals exposed to particulate matter. **a** Body weight before and after ovariectomy ($P = 0.657$). **b** Percentage of body weight gain during the first 12 weeks, before ovariectomy ($P = 0.680$). **c** Percentage of body weight gain from the 12th to the 24th week, after ovariectomy ($P = 0.023$; $F_{3,20} = 3.91$) * vs. CTRL. Data are presented as mean ± SEM. $n = 5$–6 per group. A two-way ANOVA with repeated measures (**a**), Student's *t* test (**b**), and a one-way ANOVA followed by a post hoc Tukey test (**c**)

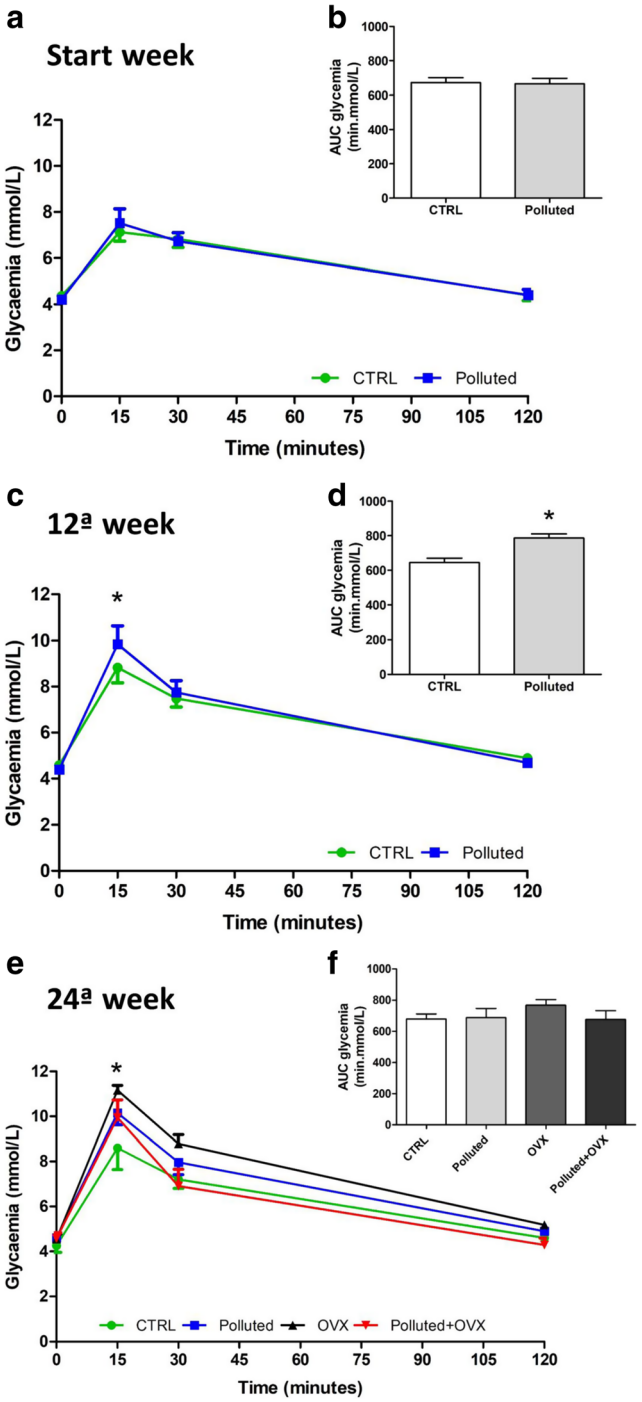

Fig. 3 The effect of reduced estrogen levels in animals exposed to particulate matter on the area under the curve in relation to the glucose tolerance test (GTT) response. **a** Baseline ($P = 0.862$). **b** AUC Baseline ($P = 0.877$; $F_{1,11} = 1.13$). **c** 12th week ($P = 0.474$). **d** AUC 12th week ($P = 0.0004$; $F_{1,11} = 1.14$) * vs CTRL. **e** 24th week ($P = 0.001$) * OVX vs CTRL**. f** AUC 24th ($P = 0.485$; $F_{3,20} = 0.84$)**.** Data presented as mean ± SEM. $n = 6$ per group. A two-way ANOVA followed by a post hoc Tukey test for GTT (**a**, **c**, and **e**), Student's t test (**b** and **d**), and a one-way ANOVA followed by a post hoc Tukey test (**f**)

The effects of reduced estrogen levels on morphometric tissue alterations

We also evaluated the influence of reduced estrogen levels in polluted animals regarding morphometric alterations in metabolic-related tissues (Table 2). The OVX and Polluted+OVX groups both experienced an increase in adiposity, and the OVX group experienced a decrease in liver mass. No alterations were observed in the rats' pancreas mass or muscle mass (the gastrocnemius and soleus muscles, respectively). The Polluted+OVX group also experienced tissue edema in the liver and lung (Table 2).

Reduced estrogen levels modify the liver redox profile and inflammatory blood markers of rats exposed to PM

The Polluted+OVX group presented a reduction in SOD activity (Fig. 4a) without changes in CAT or lipoperoxidation levels (Fig. 4b, c, respectively). Additionally, since the liver CAT activity results showed a systematic decrease from the left bars (CTRL) to the right bars (Polluted+OVX), we supposed a decrease in estrogen levels is correlated with the decrease in liver CAT activity. Although there were no differences in liver CAT activity among the groups ($P = 0.124$), there is a linear trend ($P = 0.021$, $r = 0.957$, evaluated by an ANOVA post hoc linear trend test) and a positive correlation between estrogen levels and CAT activity ($r = 0.579$, $P = 0.0059$). When analyzing intragroup correlations between estrogen and oxidative stress variables, in the Polluted+OVX group, we found that a decrease in estrogen levels is associated with a decrease in CAT activity ($r = 0.927$, $P = 0.023$) and an increase in lipid peroxidation levels in the liver ($r = 0.977$, $P = 0.004$).

We found no alterations in plasma IL-6 levels (Fig. 5a). However, OVX and particles associated with OVX decreased plasma interleukin-10 levels (Fig. 5b) and increased the IL-6/IL-10 ratio (Fig. 5c). The interventions did not modify the cytokine content in liver homogenates (Fig. 5d–f). We also found that IL-6 levels were negatively correlated with estrogen levels in the OVX group ($r = -0.981$, $P = 0.0031$). Neutrophil levels and neutrophil/lymphocyte ratios were increased in the Polluted+OVX group at the end of the 24-week study (Table 3).

Reduced levels of estrogen were associated with PM and increased liver iHSP70 but not modified plasma eHSP70 levels

The heat-shock response (HSR) is performed by proteins in the HSP70 family, such as HSP72 (72-kDa, inducible isoform) and HSP73 (73-kDa, constitutive isoform), which constitute the total HSP70 content. The Polluted+

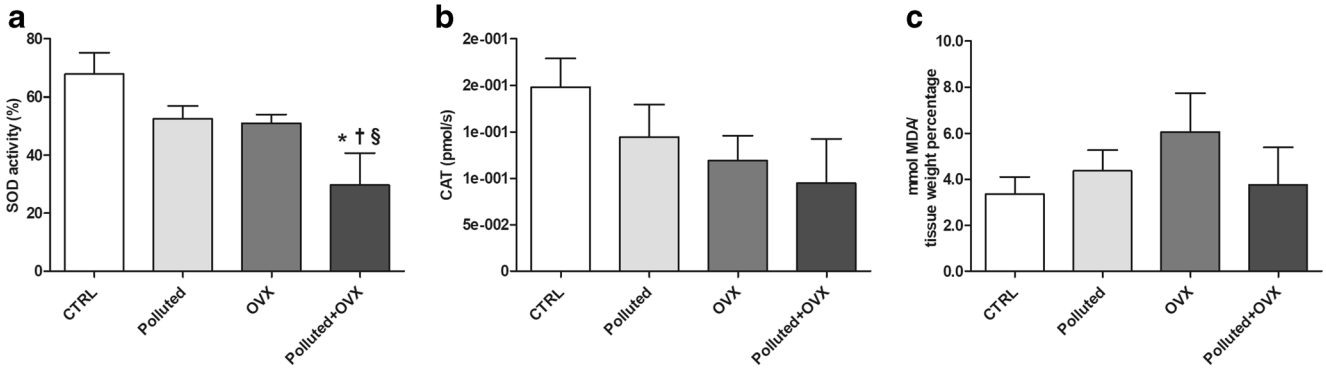

Fig. 4 The effect of reduced estrogen levels on the liver redox profile of animals exposed to particulate matter pollution. **a** SOD activity ($P = 0.0005$, $F_{3,20} = 9.34$) * vs CTRL, † vs Polluted, § vs OVX. **b** CAT activity ($P = 0.124$, $F_{3,19} = 2.17$). **c** Lipoperoxidation ($P = 0.452$, $F_{3,16} = 0.92$). Data expressed as mean ± SEM. $n = 5$–6 per group. A one-way ANOVA followed by a post hoc Tukey test

OVX group presented an increase in liver-inducible iHSP70 (iHSP72) and HSP70 total levels when compared with the CTRL group (Fig. 6a). None of the interventions modified plasma HSP70, as well as the extra-to-intracellular HSP70 ratio regarding the liver as demonstrated by the H-index values (Fig. 6b, c).

Discussion

In our study, ovariectomy promoted increased adiposity gain, reflected in increased body weight. Ovariectomized rats also presented with a pro-inflammatory profile and an altered heat-shock response in the liver when exposed to particle pollution. The data indicate that low estrogen levels represent a vulnerability to environmental air pollution challenges. Our study supports the hypothesis that menopausal women are at risk of developing metabolic diseases and that the risk increases with environmental air pollution exposure.

In our study, the animals were ovariectomized at 5 months of age; at the end of the study, all the animals were 8 months of age, and the non-ovariectomized groups presented hormonal levels characteristic of the estrus phase of the rat cycle (the mean 17β-estradiol level in the sham-operated groups was 34.1 pg/mL). The ovariectomy promoted a 24% reduction in these hormonal levels (the mean 17β-estradiol level in the ovariectomized groups was 25.9 pg/mL). Irregular estrous cycles in rodents are characteristic of laboratory rodents with initiation occurring at approximately 8 months of age (Brinton 2014), whereas acyclicity begins in most laboratory rats between 12 and 16 months (Finch et al. 2014). Also, 60–70% of the aging rodents spontaneously transition into a polyfollicular anovulatory state of constant estrus characterized by sustained levels of plasma 17β-estradiol (Brinton 2014). The stages of reproductive senescence described above, from regular cycling to irregular cycling and then to acyclicity, are similar in humans and rodents. Although the transition is of shorter duration in rodents, it is characterized by multiple features found in humans, which include a decline in follicles, irregular cycling, steroid hormone fluctuations, and irregular fertility. Thus, if our ovariectomy occurred moderately early in the life cycle of the rat, it may be not representative of a senescence rat age; however, the age of the rats at the end of the study and the duration of low estrogen levels may adequately represent metabolic dysfunction (as observed by adiposity in our data) and changes in temperature regulation, which may affect the heat-shock response (Miragem et al. 2017), that typically occur 3–5 weeks after an ovariectomy, representing preclinical models of human menopause (Brinton 2014).

Table 1 The effects of reduced estrogen levels on the biochemical profile of rats exposed to PM

Parameter	CTRL	Polluted	OVX	Polluted+OVX	*P* value
Glycemia (mmol/L)	4.3 ± 0.3	4.2 ± 0.1	4.6 ± 0.2	4.6 ± 0.3	*0.382* ($F_{3,20} = 1.07$)
Triacylglycerol (mg/dl)	120.3 ± 49.7	114.3 ± 42.9	126.2 ± 19.8	119.0 ± 9.0	*0.958* ($F_{3,20} = 0.10$)
Total cholesterol (mg/dl)	59.2 ± 3.5	61.3 ± 3.6	*75.8 ± 6.6**	*76.7 ± 3.9**	*0.020* ($F_{3,20} = 4.07$)
HDL-cholesterol (mg/dl)	22.5 ± 1.7	27.3 ± 3.4	25.8 ± 0.8	26.8 ± 1.2	*0.349* ($F_{3,20} = 1.16$)
LDL-cholesterol (mg/dl)	16.0 ± 2.8	15.3 ± 3.8	24.8 ± 7.6	26.0 ± 3.7	*0.082* ($F_{3,17} = 1.64$)
Liver triglycerides (g/100 g tissue)	2.5 ± 0.6	2.8 ± 0.6	3.6 ± 0.4	3.5 ± 0.6	*0.479* ($F_{3,19} = 0.85$)

Data expressed as mean ± SEM. *$P < 0.05$ vs. CTRL. vs CTRL and OVX"?>. One-way ANOVA followed by post hoc Tukey test. $n = 5$–6 per group

Table 2 The effects of reduced estrogen levels on morphometric tissue alterations and tissue edema in rats exposed to PM

Parameter	CTRL	Polluted	OVX	Polluted+OVX	*P* value
White adipose tissue	0.91 ± 0.17	1.03 ± 0.15	*1.39 ± 0.11**	*1.19 ± 0.20**	*0.019* ($F_{3,19} = 2.29$)
Liver	2.60 ± 0.08	2.60 ± 0.08	*2.19 ± 0.06**	2.29 ± 0.09	*0.002* ($F_{3,20} = 6.68$)
Pancreas	0.28 ± 0.03	0.29 ± 0.04	0.24 ± 0.02	0.23 ± 0.02	*0.434* ($F_{3,20} = 0.95$)
Gastrocnemius	1.24 ± 0.05	1.28 ± 0.03	1.32 ± 0.12	1.24 ± 0.04	*0.807* ($F_{3,20} = 0.32$)
Soleus	0.09 ± 0.005	0.08 ± 0.003	0.07 ± 0.003	0.08 ± 0.005	*0.059* ($F_{3,20} = 2.09$)
Liver edema	29.6 ± 0.3	30.3 ± 0.3	*31.3 ± 0.2**	*31.5 ± 0.5**	*0.001* ($F_{3,20} = 7.93$)
Lung edema	17.3 ± 0.4	18.8 ± 0.5	19.4 ± 0.3	*20.2 ± 0.7**	*0.008* ($F_{3,20} = 5.16$)

Percentage (%) of the tissue weight/body weight ratio. Data expressed as mean ± SEM. *$P < 0.05$ vs. CTRL. $n = 5$–6 per group. A one-way ANOVA followed by a post hoc Tukey test

Ovariectomized rats experienced an increase in body weight and adiposity. Sex hormones, including the decline in estrogen levels due to ovariectomy, strongly influence body fat distribution and adipocyte differentiation (Min 2018). This decrease, which is also observed in menopausal women, is associated with a loss of subcutaneous fat and an increase in abdominal fat, evidencing why menopausal women are three times more likely to develop obesity and metabolic syndrome abnormalities than premenopausal women (Eshtiaghi et al. 2010; Lizcano and Guzmán 2014), as observed in the lipid profiles in our OVX and Polluted+OVX groups.

Estrogen deficiency was able to promote hepatic steatosis (Quinn et al. 2018) in the same way these effects are produced by the consumption of high-fat (HF) diets in studies. However, exposure to $PM_{2.5}$ induces hepatic steatosis and hypertriglyceridemia in normal chow-fed mice but attenuates hepatic steatosis and hyperlipidemia in HF-fed mice (Qiu et al. 2017). We found decreased hepatic mass only in ovariectomized animals and edema in the liver tissue of ovariectomized animals regardless of pollution exposure. Cellular lesions, promoted by low estradiol levels, can lead to cellular edema or fat accumulation (i.e., steatosis; Oliveira et al. 2018), which

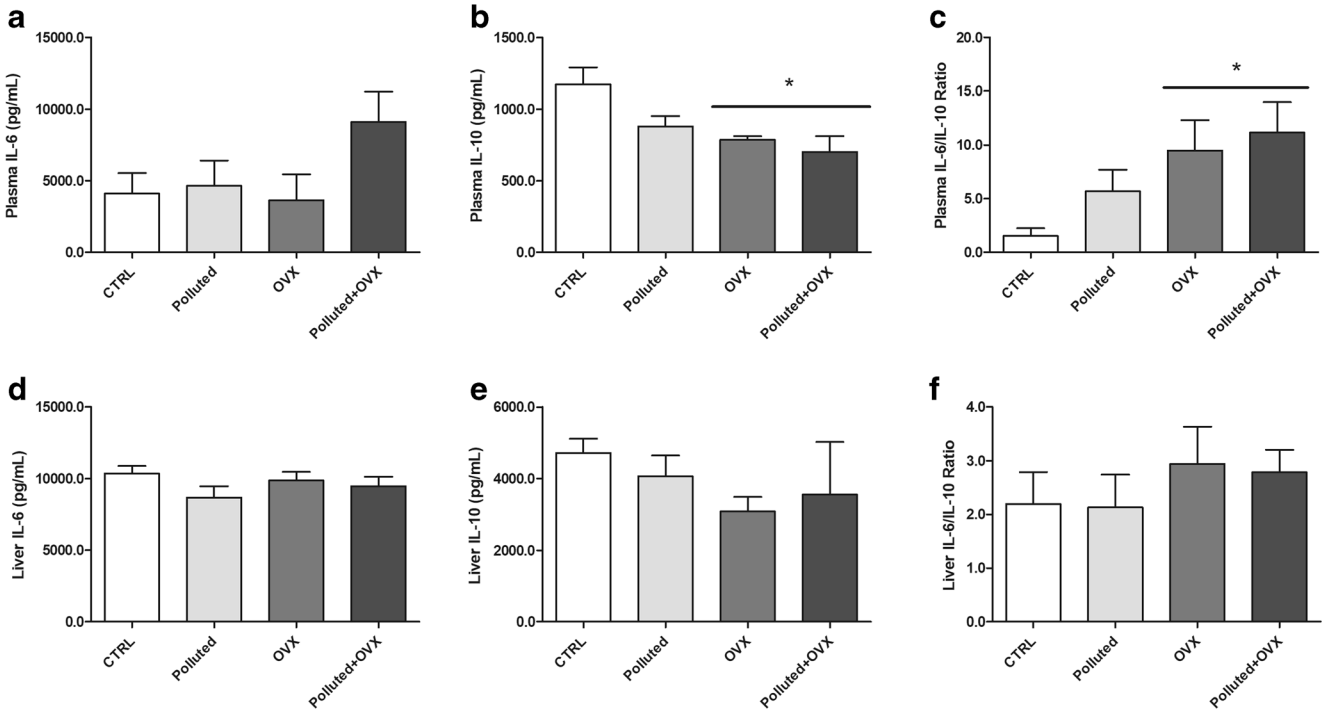

Fig. 5 The effect of reduced estrogen levels on the plasma and liver interleukin-6, interleukin-10, and the IL-6/IL-10 ratio at the 24ª week in animals exposed to particulate matter pollution. **a** Interleukin-6 ($P = 0.228$, $F_{3,13} = 1.64$). **b** Interleukin-10 ($P = 0.010$, $F_{3,14} = 5.55$) * vs CTRL. **c** IL-6/IL-10 ratio ($P = 0.044$, $F_{3,11} = 3.75$) * vs CTRL. **d** Liver interleukin-6 ($P = 0.346$, $F_{3,15} = 1.19$). **e** Liver interleukin-10 ($P = 0.181$, $F_{3,15} = 1.84$). **f** Liver IL-6/IL-10 ratio ($P = 0.696$, $F_{3,16} = 0.486$). Data expressed as mean ± SEM. $n = 3$–6 per group. A one-way ANOVA followed by a post hoc Tukey test

Table 3 Effects of reduced estrogen levels on the hematological profile of rats exposed to PM

Cells count	CTRL	Polluted	OVX	Polluted+OVX	*P* value
RBC (10^6/mm^3)	2.5 ± 0.2	2.5 ± 0.1	2.8 ± 0.2	2.7 ± 0.1	0.566 ($F_{3,20}$ = 0.69)
WBC (10^3/mm^3)	0.9 ± 0.03	1.1 ± 0.22	1.3 ± 0.07	1.1 ± 0.14	0.336 ($F_{3,20}$ = 1.19)
Lymphocytes	83.0 ± 0.7	80.8 ± 1.3	81.8 ± 1.7	78.0 ± 1.1	0.061 ($F_{3,20}$ = 2.88)
Neutrophils	11.2 ± 0.5	12.7 ± 1.3	12.5 ± 1.4	*15.5 ± 1.2**	*0.014* ($F_{3,20}$ = 5.41)
Monocytes	5.8 ± 0.3	6.5 ± 0.2	5.7 ± 0.4	6.5 ± 0.2	*0.137* ($F_{3,20}$ = 2.06)
Platelets	227 ± 29	214 ± 27	238 ± 16	251 ± 19	0.722 ($F_{3,20}$ = 0.44)
Other blood components					
Hemoglobin (Hgb) (g/dL)	4.7 ± 0.5	4.9 ± 0.3	5.2 ± 0.3	5.1 ± 0.1	0.697 ($F_{3,20}$ = 0.48)
Hematocrit (%)	13.3 ± 1.2	13.4 ± 0.7	14.6 ± 1.0	14.5 ± 0.4	0.642 ($F_{3,20}$ = 0.56)
Mean corpuscular volume (Fl)	53.3 ± 0.7	54.0 ± 0.4	53.3 ± 0.4	53.2 ± 0.5	0.650 ($F_{3,20}$ = 0.55)
Mean corpuscular Hgb (pg)	18.7 ± 0.5	19.6 ± 0.5	18.5 ± 0.2	18.8 ± 0.2	0.220 ($F_{3,20}$ = 1.60)
Mean corpuscular Hgb conc. (%)	35.6 ± 0.4	36.2 ± 0.9	35.2 ± 0.5	35.1 ± 0.1	0.435 ($F_{3,20}$ = 0.95)
Random distribution of RBC (%)	13.0 ± 0.3	13.3 ± 0.3	13.7 ± 0.4	13.1 ± 0.6	0.675 ($F_{3,20}$ = 0.51)
Mean platelet volume (10^3/mm^3)	7.4 ± 0.5	7.3 ± 0.5	7.0 ± 01	6.5 ± 0.3	0.372 ($F_{3,20}$ = 1.10)
Neutrophil/lymphocyte ratio	0.13 ± 0.01	0.16 ± 0.02	0.15 ± 0.02	*0.20 ± 0.02**	*0.049* ($F_{3,20}$ = 4.38)
Platelet/lymphocyte ratio	2.72 ± 0.3	2.64 ± 0.3	2.92 ± 0.2	3.22 ± 0.2	0.464 ($F_{3,20}$ = 0.88)

Data expressed as mean ± SEM. *$P < 0.05$ vs. CTRL. $n = 6$ per group. A one-way ANOVA followed by a post hoc Tukey test

occur when the cell is unable to maintain ionic homeostasis. Air pollution may be attenuating the development of hepatic steatosis and severe lipid abnormalities via the autophagy mechanism (Qiu et al. 2017).

Several liver dysfunctions significantly alter lipid metabolism. Lipids are necessary components that control cellular functions and homeostasis, and the liver plays an essential role in lipid metabolism, as well as several stages of lipid synthesis and transportation (Ghadir et al. 2010). Our data show that the effects of ovariectomy on the liver promoted an increase in total cholesterol levels. Since estrogens and estrogen receptors regulate various aspects of glucose and lipid metabolism (Lizcano and Guzmán 2014), reduced estrogen levels promote hypercholesterolemia.

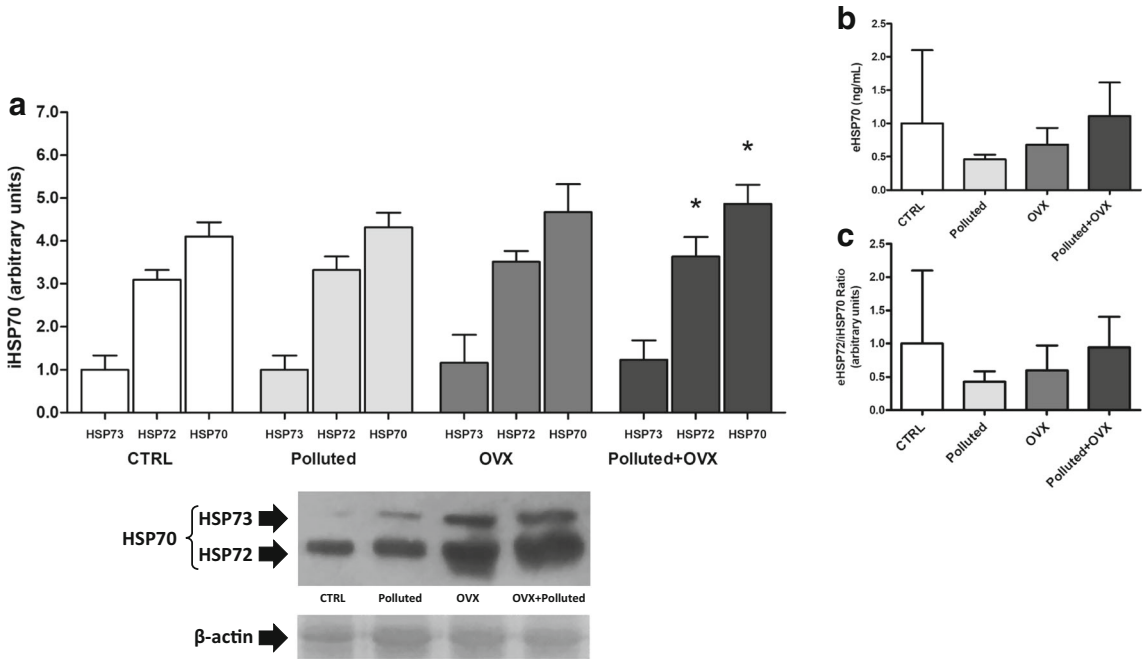

Fig. 6 The effect of low estrogen levels on hepatic iHSP70 expression, eHSP72 levels, and H-index ([eHSP72]/[iHSP70] ratio) values in animals exposed to particulate matter pollution. **a** Liver HSP73 ($P = 0.882$, $F_{3,7} = 0.21$), HSP72 ($P = 0.046$, $F_{3,16} = 2.62$), HSP70 ($P = 0.047$, $F_{3,1\ 6} = 2.77$) (arbitrary units) * vs CTRL. **b** eHSP70 ($P = 0.647$, $F_{3,12} = 0.57$). **c** [eHSP72]/[iHSP70] ratio ($P = 0.727$, $F_{3,12} = 0.44$). Data expressed as mean ±SD. $n = 3$–5 per group. A one-way ANOVA followed by a post hoc Tukey test

While ovariectomy promoted direct effects on tissues that are related to metabolism, such as the liver, and consequently, in lipid metabolism, particulate matter pollution can directly affect lung tissue, causing pulmonary tissue edema. Exposure to PM can promote tissue injury by the direct effects of particle components, leading to oxidative and cellular stress, and by indirect effects, triggering the production of pro-inflammatory mediators, with consequent systemic low-grade inflammation (Goettems-Fiorin et al. 2016; Hoffmann et al. 2009; Miller et al. 2012).

Estrogen is known to prevent inflammatory gene transcription induced by inflammatory agents by inhibiting NF-κB intracellular transport, an immediate-early event in the inflammatory signaling cascade (Ghisletti et al. 2005; Pelekanou et al. 2016). In our study, estrogen privation promoted a decrease in anti-inflammatory defense, with a reduction in IL-10 levels and an increase in the pro-inflammatory profile as indicated by the IL-6/IL-10 ratio. The decrease in plasma IL-10 may be causing changes in the leukocyte profile. Interleukin-10 is a crucial inhibitor of many aspects of the inflammatory response, primarily by inhibiting macrophage proliferation (O'Farrell et al. 1998). Once IL-10 can regulate their proliferation and, thus, the numbers of inflammatory cells and reduced IL-10 levels may result in increased neutrophilia and an increased ratio of neutrophils and lymphocytes (NLR). NLR is a simple parameter used to assess the inflammatory status of a subject and has the potential to be a sensitive prognostic marker (Faria et al. 2016). Air pollution is known to promote low-grade chronic inflammation, which can lead to severe cardiometabolic dysfunction in the long term (Sun et al. 2015; Wang et al. 2018). Furthermore, the relationship between estrogens and metabolism is reciprocal since the metabolic control favored by estrogens avoids the establishment of metabolic inflammation (Monteiro et al. 2014), although these effects cannot yet be evidenced directly in tissues related to metabolism, such as in the liver. The adiposity, liver edema, hypercholesterolemia, neutrophil-lymphocyte ratio (NLR), interleukins ratio (IL-6/IL-10), and increase in iHSP72 levels make it clear that the progression of these factors will further aggravate the glucose intolerance observed in particle-exposed animals, predisposing them to metabolic dysfunction, a condition that will develop into type 2 diabetes in later phases, primarily under low levels of estrogen as observed postmenopause.

In our study, we found a decrease in liver antioxidant enzyme activity (Fig. 4), an increase in the plasma pro-inflammatory profile (Fig. 5), and an increase in liver iHSP70 expression in the Polluted+OVX group. Decreased estrogen levels were also correlated with increased lipid peroxidation levels and lower antioxidant enzyme activity. Estrogen deficiency (Escalante-Gómez et al. 2009) and metabolic changes due to its decline predispose the female organism to an increase in the production of reactive oxygen species (ROS) and reactive nitrogen species (NR), resulting in increased oxidative stress (OS; Crist et al. 2009). Oxidative stress may promote hepatic cellular stress, and at an early stage, the liver is able to evoke the heat shock response (HSR) and, consequently, increase the levels of iHSP70 to maintain homeostasis (Ludwig et al. 2014). Thus, the observed increase in liver iHSP72 content may represent an essential endogenous response to cellular stress and is sensitive to the occurrence of OS (Nakhjavani et al. 2010), related to the availability of estrogen (Hou et al. 2010). Thus, despite the decrease in antioxidant defense (SOD) in the Polluted+OVX group, the increase in the levels of iHSP70 as a cytoprotective response may avoid liver damage and dysfunction. Studies show that the absence of estrogens in rat favors fat accretion in the liver, which is significantly amplified by a high-fat diet (Shinoda and Lavoie 2007). However, our study demonstrated no difference in hepatic triglycerides profile, which may be related to the defense of heat-shock proteins.

It is well known that HSP70 expression is regulated by HSF1, which is, in turn, redox-regulated due to highly conserved cysteines (Ahn and Thiele 2003), in which HSP70 expression is induced following the oxidation of cysteine-containing GSH molecules. HSP70 expression in the liver represents a protective redox-mediated HSR induction by nitric oxide free radicals in rat hepatocytes that occurs when these cells are treated with a pro-inflammatory cytokine, a process mediated by nitric oxide signaling (Kim et al. 1997). Furthermore, decreased estrogen levels diminished the suppressive effect of this hormone in hypothalamic areas involved in thermoregulation, notably the infundibular nucleus in humans and the arcuate nucleus in other mammals, specifically in the kisspeptin-neurokinin B-dynorphin neurons (KNDy). The consequent rise in KNDy neuron activity leads to the stimulation of NO and HSP70 production, both directly and indirectly, via neuropeptide Y (NPY)-secreting neurons as a contra-regulatory action against the decrease in estrogen hormonal regulation (Miragem et al. 2017). Thus, ovariectomy may increase KNDy neuron function and, thus, enhance NF-kB activity, predisposing the pro-inflammatory state observed in our study. Finally, liver HSP70 may be associated with adrenergic stimulation secondary to long-term estrogen deprivation (Freedman and Neurosciences 2015; Krause and Nakajima 2014) and should confer cytoprotection due to the stimulatory nature of adrenergic signaling over HSR and HSP70 production in the liver.

Although the H-index ([eHSP72]/[iHSP70] ratio) can reveal the context of an inflammatory process (Heck et al. 2017) and insulin resistance state (Krause et al. 2015), in our study, H-index was not altered by low levels of estrogen and exposure to particles. Our previous studies suggest that acute exposure to ROFA suspension at higher doses (a 1.5-fold dose—375 μg/50 μL) was able to produce an increase in plasma eHSP70 levels (primarily the 72-kDa inducible form) and

promoted alterations in plasma oxidative stress (Baldissera et al. 2018), although in chronic exposure studies, there was no increase in eHSP70 levels (Goettems-Fiorin et al. 2016; Mai et al. 2017). As estrogen is a physiological inducer of the heat-shock response, some estrogen-based protective effects could be related to its anti-inflammatory action via HSP70 expression. Studies have shown that in short-term estrogen deprivation, the HS response seems to be preserved, which an efficient HSP70-based anti-inflammatory response, thus avoiding oxidative stress and tissue damage (Miragem et al. 2015). Furthermore, in contrast with high-fat diet animal models with severe metabolic disease (Bruxel et al. 2019; Goettems-Fiorin et al. 2016) or human obesity studies (Rodrigues-Krause et al. 2012), which found an altered H-index, in our study, we did not find an imbalance in eHSP70 and iHSP70 levels. This difference may be due to the moderate nature of our experimental challenges, which promote only moderate biometric and metabolic effects without a greater increase in insulin resistance and obesity, in comparison with more aggressive metabolic disease studies.

While our study evidenced that ovariectomy promotes several metabolic, oxidative, pro-inflammatory, and heat-shock balance changes in the liver and predisposes female rats to fine particulate matter exposure effects, new studies may provide a more complete description of the effects of menopause and air pollution exposure on metabolic profiles. Thus, future animal studies that aim to investigate insulin levels and the insulin signaling pathway in the liver, lipogenesis and fatty acid oxidation enzymes metabolism, other hormones involved in metabolism, such as leptin, as well as a histopathological analysis of liver and adipose tissue are recommended. Studies involving hormonal replacement may help prove the role of estrogen levels in the effects observed in our study.

Conclusion

Ovariectomy promotes biometric and metabolic effects that, under environmental air pollution exposure conditions, represent an increased susceptibility to an oxidative stress state, a pro-inflammatory profile, and an altered liver heat-shock response. Our data indicate that alterations in the reproductive system predispose female organisms to particulate matter air pollution effects.

Acknowledgments The authors would like to thank colleagues from the Laboratory of Atmospheric Pollution (UFCSPA), all students from the Research Group in Physiology (UNIJUI), and Prof. Paulo Ivo Homem de Bittencourt Jr. from the Laboratory of Cellular Physiology (UFRGS) for their technical support.

Authors' contributions PBGF completed all the experiments described in this manuscript. LCCB, JBS, PTF, and LMS performed the biometric and metabolic profile procedures and performed the administration of particles in the rats used in this study. LCCB, JBS, and LMS performed the experiments on oxidative stress parameters. JBS and LMS performed the Western blot analyses. MNF performed the hematological procedures. TGH performed eHSP70, cytokine, and eHSP70/iHSP70 ratio procedures. All authors were involved in analyzing the results. TGH and PBGF co-wrote the manuscript. Figure 1 was designed by TGH and PBGF. TGH, MSL, and CRR designed the study and provided experimental advice and helped with manuscript revision. All the authors had final approval of the submitted and published versions.

Funding This work was financially supported by the Regional University of Northwestern Rio Grande do Sul State (UNIJUI) and Federal University of Health Sciences of Porto Alegre (UFCSPA), as well as by grants from the Research Support Foundation of the State of Rio Grande do Sul (#ARD/PPP/FAPERGS/CNPq 08/2014, process 16/2551-0000196-0 to TGH) and the Brazilian National Council for Scientific and Technological Development (CNPq) (#MCTI/CNPq N° 01/2016 – CNPq, process 407329/2016-1 to TGH). LCCB was the recipient of a scholarship from the Coordination for the Improvement of Higher Education Personnel (CAPES), and JBS, LMS, and PTS were the recipients of a scholarship from FAPERGS and CNPq.

Data availability The data used to support the findings of this study are available from the corresponding authors upon request.

Compliance with ethical standards

Competing interests The authors declare that they have no competing interests.

References

Aebi H (1984) Catalse in vitro. Methods Enzymol 105:121–126

Ahn S, Thiele DJ (2003) Redox regulation of mammalian heat shock factor 1 is essential for Hsp gene activation and protection from stress. Genes Dev 17(4):516-28. https://doi.org/10.1101/gad.1044503.ors

Baldissera FG, Bender A, Sulzbacher MM (2018) Subacute exposure to residual oil fly ash (ROFA) increases eHSP70 content and extracellular-to-intracellular HSP70 ratio : a relation with oxidative stress markers. Cell Stress Chaperones 23(6):1185-1192. https://doi.org/10.1007/s12192-018-0924-z

Benedusi V, Martini E, Kallikourdis M, Villa A (2014). Ovariectomy shortens the life span of female mice. Oncotarget 10;6(13):10801-11

Bradford MM (1976) A rapid and sensitive method for the quantitation of microgram quantities of protein utilizing the principle of protein-dye binding. Anal Biochem 72:248–254. https://doi.org/10.1016/0003-2697(76)90527-3

Brinton RD (2014) Minireview : translational animal models of human menopause : challenges and emerging opportunities. Endocrinology 153(8):3571-8. https://doi.org/10.1210/en.2012-1340

Bruxel MA, Tavares AMV, Zavarize Neto LD, de Souza Borges V, Schroeder HT, Bock PM, Rodrigues MIL, Belló-Klein A, Homem de Bittencourt PI (2019) Chronic whole-body heat treatment relieves atherosclerotic lesions, cardiovascular and metabolic abnormalities, and enhances survival time restoring the anti-inflammatory and anti-senescent heat shock response in mice. Biochimie 156:33–46. https://doi.org/10.1016/J.BIOCHI.2018.09.011

Buege J, Aust S (1978) Microssomal lipid peroxidation. Methods Enzymol 52:302–309

Cangeri Di Naso F, Rosa Porto R, Sarubbi Fillmann H, Maggioni L, Vontobel Padoin A, Jacques Ramos R, Corá Mottin C, Bittencourt A, Anair Possa Marroni N, Ivo Homem de Bittencourt P (2015) Obesity depresses the anti-inflammatory HSP70 pathway, contributing to NAFLD progression. Obesity 23:120–129. https://doi.org/10.1002/oby.20919

Crist BL, Alekel DL, Ritland LM, Hanson LN, Genschel U, Reddy MB (2009) Association of oxidative stress, iron, and centralized fat mass in healthy postmenopausal women. J Women's Health 18:795–801. https://doi.org/10.1089/jwh.2008.0988

EPA (2010) http://www.epa.gov/OCEPAterms/sterms.html [WWW Document]. URL http://www.epa.gov/OCEPAterms/sterms.html. Accessed on: . Accessed 12 Nov 2018.

Escalante-Gómez C, Quesada-Mora S, Zeledón-Sánchez F, Gómez CE (2009) Perfil oxidativo de la mujer menopáusica: Papel de los estrógenos en la prevención y tratamiento de las enfermedades (Oxidative Profile of the Menopausal Woman: Estrogensol in the Prevention and Treatment of Diseases). Acta Med Costarric 51:206–212

Eshtiaghi R, Esteghamati A, Nakhjavani M (2010) Menopause is an independent predictor of metabolic syndrome in Iranian women. Maturitas 65:262–266. https://doi.org/10.1016/j.maturitas.2009.11.004

Faria SS, Fernandes PC, Silva MJB, Lima VC, Fontes W, Freitas R, Eterovic AK, Forget P (2016) The neutrophil-to-lymphocyte ratio: a narrative review. Ecancermedicalscience 10:1–12. https://doi.org/10.3332/ecancer.2016.702

Finch CE, Felicio LS, Mobbs CV, Nelson JF (1984). Ovarian and steroidal influences on neuroendocrine. Endocr Rev 5(4):467-97

Freedman RR (2014) Menopausal hot flashes: mechanisms, endocrinology, treatment. J Steroid Biochem Mol Biol 142:115-20. https://doi.org/10.1016/j.jsbmb.2013.08.010

Ghadir MR, Riahin AA, Havaspour A, Nooranipour M, Habibinejad AA (2010) The relationship between lipid profile and severity of liver damage in cirrhotic patients. Hepat Mon 10:285–288

Ghisletti S, Meda C, Maggi A, Vegeto E (2005) 17beta-estradiol inhibits inflammatory gene expression by controlling NF- κ B intracellular localization. Mol Cell Biol 25(8):2957-68. https://doi.org/10.1128/MCB.25.8.2957

Goettems-Fiorin PB, Grochanke BS, Baldissera FG, dos Santos AB, Homem de Bittencourt PI, Ludwig MS, Rhoden CR, Heck TG (2016) Fine particulate matter potentiates type 2 diabetes development in high-fat diet-treated mice: stress response and extracellular to intracellular HSP70 ratio analysis. J Physiol Biochem 72:643–656. https://doi.org/10.1007/s13105-016-0503-7

Heck TG, Scomazzon SP, Nunes PR, Schöler CM, da Silva GS, Bittencourt A, Faccioni-Heuser MC, Krause M, Bazotte RB, Curi R, Homem de Bittencourt PI (2017) Acute exercise boosts cell proliferation and the heat shock response in lymphocytes: correlation with cytokine production and extracellular-to-intracellular HSP70 ratio. Cell Stress Chaperones 22:271–291. https://doi.org/10.1007/s12192-017-0771-3

Heck TG, Brendler P, Fiorin G, Frizzo MN, Ludwig MS (2017) Fine Particulate Matter (PM2.5) Air Pollution and Type 2 Diabetes Mellitus (T2DM): When Experimental Data Explains Epidemiological Facts. IntechOpen, Diabetes and Its Complications, Edited by Ahmed RG https://doi.org/10.5772/intechopen.70668

Hoffmann B, Moebus S, Dragano N, Stang A, Möhlenkamp S, Schmermund A, Memmesheimer M, Bröcker-Preuss M, Mann K, Erbel R, Jöckel K-H (2009) Chronic residential exposure to particulate matter air pollution and systemic inflammatory markers. Environ Health Perspect 117:1302–1308. https://doi.org/10.1289/ehp.0800362

Hou Y, Wei H, Luo Y, Liu G (2010) Modulating expression of brain heat shock proteins by estrogen in ovariectomized mice model of aging. Exp Gerontol 45:323–330. https://doi.org/10.1016/j.exger.2009.10.006

Kim Y, Vera ME De, Watkins SC, Billiar TR (1997) Nitric oxide protects cultured rat hepatocytes from tumor necrosis factor-alpha-induced apoptosis by inducing heat shock protein 70 expression. J Biol Chem 272(2):1402-11

Kolberg A, Rosa TG, Puhl MT, Scola G, Janner DDR, Maslinkiewicz A, Lagranha DJ, Heck TG, Curi R, Homem De Bittencourt PI (2006) Low expression of MRP1/GS-X pump ATPase in lymphocytes of Walker 256 tumour-bearing rats is associated with cyclopentenone prostaglandin accumulation and cancer immunodeficiency. Cell Biochem Funct 24:23–39. https://doi.org/10.1002/cbf.1290

Krause MS, Nakajima ST (2014) Hormonal and Nonhormonal Treatment of Vasomotor Symptoms. Obstet Gynecol Clin North Am 42(1):163-79. https://doi.org/10.1016/j.ogc.2014.09.008

Krause M, Heck TG, Bittencourt A, Scomazzon SP, Newsholme P, Curi R, Homem de Bittencourt PI (2015) The chaperone balance hypothesis: the importance of the extracellular to intracellular HSP70 ratio to inflammation-driven type 2 diabetes, the effect of exercise, and the implications for clinical management. Mediat Inflamm 2015:249205. https://doi.org/10.1155/2015/249205

Lee MO (1929) Determination of the surface area of the white rat with its application to the expression of metabolic results. Am J Physiol – Leg Content 89:24–33

Liu C, Xu X, Bai Y, Wang TY, Rao X, Wang A, Sun L, Ying Z, Gushchina L, Maiseyeu A, Morishita M, Sun Q, Harkema JR, Rajagopalan S (2014) Air pollution-mediated susceptibility to inflammation and insulin resistance: influence of CCR2 pathways in mice. Environ Health Perspect 122:17–26. https://doi.org/10.1289/ehp.1306841

Lizcano F, Guzmán G (2014) Estrogen deficiency and the origin of obesity during menopause. Biomed Res Int 2014:1–11. https://doi.org/10.1155/2014/757461

Ludwig MS, Minguetti-Câmara VC, Heck TG, Scomazzon SP, Nunes PR, Bazotte RB, Homem de Bittencourt PI (2014) Short-term but not long-term hypoglycaemia enhances plasma levels and hepatic expression of HSP72 in insulin-treated rats: an effect associated with increased IL-6 levels but not with IL-10 or TNF–α. Mol Cell Biochem 397:97–107. https://doi.org/10.1007/s11010-014-2176-2

Mai AS, Dos Santos AB, Beber LCC, Basso RDB, Sulzbacher LM, Goettems-Fiorin PB, Frizzo MN, Rhoden CR, Ludwig MS, Heck TG (2017) Exercise training under exposure to low levels of fine particulate matter: effects on heart oxidative stress and extra-to-intracellular HSP70 ratio. Oxidative Med Cell Longev 2017:1–13. https://doi.org/10.1155/2017/9067875

Marklund S, Marklund G (1974) Involvement of the superoxide anion radical in the autoxidation of pyrogallol and a convenient assay for superoxide dismutase. Eur J Biochem 47:469–474. https://doi.org/10.1111/j.1432-1033.1974.tb03714.x

Medeiros N et al (2004) Acute pulmonary and hematological effects of two types of particle surrogates are influenced by their elemental composition Environ Res 95(1):62-70. https://doi.org/10.1016/j.envres.2003.07.007

Miller MR, Shaw C a, Langrish JP (2012) From particles to patients: oxidative stress and the cardiovascular effects of air pollution. Futur Cardiol 8:577–602. https://doi.org/10.2217/fca.12.43

Min W (2018) The decline of whole-body glucose metabolism in ovariectomized rats ☆. Exp Gerontol 113:106–112. https://doi.org/10.1016/j.exger.2018.09.027

Miragem AA, Ludwig MS, Heck TG, Baldissera FG, dos Santos AB, Frizzo MN, Homem de Bittencourt PI (2015) Estrogen deprivation does not affect vascular heat shock response in female rats: a comparison with oxidative stress markers. Mol Cell Biochem 407:239–249. https://doi.org/10.1007/s11010-015-2472-5

Miragem AA, Ivo P, Bittencourt H De (2017) Nitric oxide-heat shock protein axis in menopausal hot flushes: neglected metabolic issues of chronic inflammatory diseases associated with deranged heat shock response. Hum Reprod Update 23(5):600-628. https://doi.org/10.1093/humupd/dmx020

Monteiro R, Teixeira D, Calhau C (2014) Estrogen signaling in metabolic inflammation. Mediat Inflamm 2014:1–20. https://doi.org/10.1155/2014/615917

Nakhjavani M, Morteza A, Khajeali L, Esteghamati A, Khalilzadeh O, Asgarani F, Outeiro TF (2010) Increased serum HSP70 levels are associated with the duration of diabetes. Cell Stress Chaperones 15:959–964. https://doi.org/10.1007/s12192-010-0204-z

North American Menopause Society (2010) Overview of menopause. Menopause Pract A Clin Guid:1–5. https://www.menopause.org/. Accessed 21 Aug 2018

O'Farrell A-M, Liu Y, Moore KW, Mui A (1998) IL-10 inhibits macrophage activation and proliferation by distinct signaling mechanisms: evidence for Stat3-dependent and -independent pathways. EMBO J 17:1006–1018

Oakes ND, Thale PG, Jacinto SM, Ljung B (2001) Exchange capacity and enhance insulin-mediated control of systemic FFA availability. Diabetes 50(5):1158-65

Oliveira MC, Campos-Shimada L, Marçal-Natali M, Ishii-Iwamoto E, Salgueiro-Pagadigorria C (2018) A Long-term estrogen deficiency in ovariectomized nice is associated with disturbances in fatty acid oxidation and oxidative stress. Revista Brasileira de Ginecologia e Obstetrícia / RBGO Gynecology and Obstetrics 40(05):251-259. https://doi.org/10.1055/s-0038-1666856

Pearson J, Bachireddy C, Shyamprasad S, Goldfine A, Brownstein J (2010) Association between fine particulate matter and diabetes prevalence in the U.S. Diabetes Care 33:2196–2201. https://doi.org/10.2337/dc10-0698

Pelekanou V, Kampa M, Kiagiadaki F, Deli A, Theodoropoulos P, Agrogiannis G, Patsouris E, Tsapis A, Castanas E, Notas G (2016) Estrogen anti-inflammatory activity on human monocytes is mediated through cross-talk between estrogen receptor ER a 36 and GPR30 / GPER1. J Leukoc Biol 99(2):333-47. https://doi.org/10.1189/jlb.3A0914-430RR

Pope CA (2000) Epidemiology of fine particulate air pollution and human health: biologic mechanisms and who's at risk? Environ Health Perspect 108:713–723. https://doi.org/10.2307/3454408

Qiu Y, Zheng Z, Kim H, Yang Z, Zhang G, Shi X, Sun F, Peng C, Ding Y, Wang A, Chen LC, Rajagopalan S, Sun Q, Zhang K (2017) Inhalation exposure to PM2.5counteracts hepatic steatosis in mice fed high-fat diet by stimulating hepatic autophagy. Sci Rep 7:1–11. https://doi.org/10.1038/s41598-017-16490-3

Quinn MA, Xu X, Ronfani M, Cidlowski JA (2018) Estrogen deficiency promotes hepatic steatosis via a glucocorticoid receptor-dependent mechanism in mice. Cell Rep 22:2601–2614. https://doi.org/10.1016/j.celrep.2018.02.041

Rettberg JR, Yao J, Brinton RD (2014) Estrogen: a master regulator of bioenergetic systems in the brain and body. Front Neuroendocrinol 35:8–30. https://doi.org/10.1016/j.yfrne.2013.08.001

Rodrigues-Krause J, Krause M, O'Hagan C, De Vito G, Boreham C, Murphy C, Newsholme P, Colleran G (2012) Divergence of intracellular and extracellular HSP72 in type 2 diabetes: does fat matter? Cell Stress Chaperones 17:293–302. https://doi.org/10.1007/s12192-011-0319-x

Sacks JD, Stanek LW, Luben TJ, Johns DO, Buckley BJ, Brown JS, Ross M (2011) Particulate matter-induced health effects: who is susceptible? Environ Health Perspect 119:446–454. https://doi.org/10.1289/ehp.1002255

Santos RD, Carvalho FG, Lima TP, Viegas RL, Faria A, Suen VM, Navarro AM, Iannetta R, Nonino CB, Marchini JS (2012) Perfil do estado de saúde de mulheres climatéricas. Med (Ribeirão Preto) 45:310–317

Schneider JG, Tompkins C, Blumenthal RS, Mora S (2006) The metabolic syndrome in women. Cardiol Rev 14:286–291. https://doi.org/10.1097/01.crd.0000233757.15181.67

Shinoda M, Lavoie J (2007) Time course of liver lipid infiltration in ovariectomized rats: impact of a high-fat diet. Maturitas 58(2):182-90. https://doi.org/10.1016/j.maturitas.2007.08.002

Sposito AC, Caramelli B, Fonseca FA, Bertolami MC, Afiune Neto A, Souza AD et al (2001) III Diretriz brasileira Sobre Dislipidemias e Prevenção da Aterosclerose do Departamento de Aterosclerose da Sociedade Brasileira de Cardiologia. Arq Bras Cardiol 8:2–19. https://doi.org/10.1590/S0066-782X2007000700002

Sun Q, Yue P, Deiuliis J a, Lumeng CN, Kampfrath T, Mikolaj MB, Cai Y, Ostrowski MC, Lu B, Parthasarathy S, Brook RD, Moffatt-Bruce SD, Chen LC, Rajagopalan S (2009) Ambient air pollution exaggerates adipose inflammation and insulin resistance in a mouse model of diet-induced obesity. Circulation 119:538–546. https://doi.org/10.1161/CIRCULATIONAHA.108.799015

Sun Z, Mukherjee B, Brook RD, Gatts GA, Yang F, Fan Z, Brook JR, Sun Q, Rajagopalan S (2015) Air-pollution and cardiometabolic diseases (AIRCMD): a prospective study investigating the impact of air pollution exposure and propensity for type II diabetes. Sci Total Environ 15;448:72-8. https://doi.org/10.1016/j.scitotenv.2012.10.087

Wang Y, Han Y, Zhu T, Li W, Zhang H (2018) A prospective study (SCOPE) comparing the cardiometabolic and respiratory effects of air pollution exposure on healthy and pre-diabetic individuals. Sci China Life Sci 61:46–56. https://doi.org/10.1007/s11427-017-9074-2

Who F (1998) Carbohydrates in human nutrition. Report of a Joint FAO/WHO ExpertConsultation. FAO Food Nutr Pap 66:1-140 https://www.who.int/nutrition/publications/nutrientrequirements/9251041148/en/. Accessed 15 September 2018

Who (2003) Health aspects of air pollution with particulate matter, ozone and nitrogen dioxide : report on a WHO working group, Bonn, Germany. 13–15 January 2003 98. https://doi.org/10.2105/AJPH.48.7.913

Xu X, Yavar Z, Verdin M, Ying Z, Mihai G, Kampfrath T, Wang A, Zhong M, Lippmann M, Chen LC, Rajagopalan S, Sun Q (2010) Effect of early particulate air pollution exposure on obesity in mice: role of p47phox. Arterioscler Thromb Vasc Biol 30:2518–2527. https://doi.org/10.1161/ATVBAHA.110.215350

Yu A, Jia G, You J, Zhang P (2018) Estimation of PM2.5 concentration efficiency and potential public mortality reduction in urban China. Int J Environ Res Public Health 15:529. https://doi.org/10.3390/ijerph15030529